iJRASET
International Journal For Research in Applied Science and Engineering Technology

INTERNATIONAL JOURNAL FOR RESEARCH

IN APPLIED SCIENCE & ENGINEERING TECHNOLOGY

Volume: 11 **Issue:** II **Month of publication:** February 2023

DOI: https://doi.org/10.22214/ijraset.2023.49149

www.ijraset.com

Call: 08813907089 | E-mail ID: ijraset@gmail.com

International Journal for Research in Applied Science & Engineering Technology (IJRASET)
ISSN: 2321-9653; IC Value: 45.98; SJ Impact Factor: 7.538
Volume 11 Issue II Feb 2023- Available at www.ijraset.com

Peristaltic Transport of a Couple Stress Fluid through a Horizontal Tapered Asymmetric Channel

J. Kamalakkannan[1], C. Dhanapal[2], M. Kothandapani[3]
[1]*Research Scholar, Research and Development Center, Bharathiar University, Coimbatore 641046, Tamilnadu, India*
[2]*Department of Science and Humanities, Adhiparasakthi College of Engineering, Kalavai 632506, Tamilnadu, India*
[3]*Department of Mathematics, University College of Engineering, Arni, Tamil Nadu 632326, Tamilnadu, India*

Abstract: ***The peristaltic transport of a Couple stress fluid in the horizontal tapered asymmetric channel is examined, concealed by long wavelength and low Reynolds number assumptions. The tapered asymmetric channel is produced due to the peristaltic motion on the walls of the non-uniform channel having alternative amplitudes and phases. Excellent velocity, pressure gradient, and stream function results have been determined. Numerical evaluation has also been found for investigating the pumping characteristics with various flow values of parameters. It has been shown that the peristaltic transport pumping decreases with an increase in non-uniform rheological parameters. Further, our conclusion is created to be very relevant to [19] when the absence of the tapered asymmetric nature of the channel and couple stress fluid parameter.***
Keywords: Couple stress fluid; Peristaltic transport; tapered asymmetric channel.

I. INTRODUCTION

Physiologists have found that peristaltic flow plays a key role in transport of fluid in many biological systems. Especially, a peristaltic mechanism may be regarded in chyme movement in the gastrointestinal tract, in transport of the ovum in female fallopian tube, in urine transport from kidney to bladder through urethra and also in industries for the transport of noxious fluid in nuclear industries, as well as in roller pumps, in blood pumps, in heart lung machine, vasomotion of small blood vessels, and many others. The problem of the mechanism of peristaltic motion has attracted the care of many detectives since the first investigation of Latham [1]. The initial mathematical model of peristalsis viewed by train of sinusoidal waves in an infinitely long symmetric channel or tube has been initially studied by Fung and Yih [2] and Shapiro et al. [3]. Later, researchers have extended a number of analytical, numerical and experimental studies of peristaltic transport of different fluids have been reported under different conditions with reference to physiological and mechanical situations (Refs. [4-11] and references therein). Undoubtedly, the most of physiological and industrial fluids including blood act as non-Newtonian fluids. Since, the observer of peristaltic motion of non-Newtonian fluids may assist to get better realizing of the biological systems. Even the latest researchers in the field are expecting for the analysis of peristaltic flows under different aspects [12-17]. It is a well known fact that, couple stress fluid is very useful in understanding several physical problems because it possesses the mechanism to illustrate rheological fluids such as blood, lubricants containing small amount of high polymer additive, liquid crystals, human blood, synovial joint, electro-rheological fluids and synthetic fluids. In this view the model formulated by Stokes [20] and represents to predict micro structural characteristics (particle size) of physiological suspensions with good precision. Mekheimer [21] studied the problem of the peristaltic transport of a couple stress fluid in a uniform and non-uniform channel. Effect of the induced magnetic field on peristaltic flow of a magneto-couple stress fluid was studied by Mekheimer [22]. His study indicates that the current density at the center of the channel is higher for a couple stress fluid than a Newtonian fluid, and it also decreases as the transverse magnetic field increases. Pandey and Chaube [23] have investigated the peristaltic transport of a couple stress fluid in a channel with compliant walls. They have determined that the mean velocity at boundaries decreases with increasing couple-stress parameter and wall damping and increases with increase of wall tension and wall elasticity. The peristaltic flow of a couple stress fluid under the effect of induced magnetic field in an asymmetric channel have been observed by Nadeem and Akram [24], It is valuable to mention that the intra uterine fluid flow in a sagittal cross-section of non-pregnant uterus caused by myometrial contractions is a peristaltic–type fluid motion. In view of the above mentioned reasons, a new mathematical/theoretical analysis of peristaltic transport of a couple stress fluid in the most generalized form of the channel mentioned as the tapered asymmetric channel is investigated. To the best of our knowledge, no endeavor has been reported yet to discuss the peristaltic flow of a couple stress fluid through in the tapered asymmetric channel under the assumptions of long wavelength and low Reynolds number. The exact solutions of velocity distribution, pressure gradient and steam function are obtained. The influence of various pertinent parameters on the flow characteristics are discussed in details with the help of graphs.

ISSN: 2321-9653; IC Value: 45.98; SJ Impact Factor: 7.538
Volume 11 Issue II Feb 2023- Available at www.ijraset.com

II. MATHEMATICAL FORMULATION

Let us examine the peristaltic motion of a Couple stress fluids over a two-dimensional non-uniform thickness *2d* with a sinusoidal wave traveling over constant speed c, asymmetric concerning its axis (see Figure 1). Let $\overline{h_1'}$ and $\overline{h_2'}$ be commonly the tapered asymmetric channel's lower and upper wall boundaries. The geometry of the tapered asymmetric channel wall properties is defined (Figure 1) as

$$\overline{h_1'}\left(\overline{x'},\overline{t'}\right)= -d-\overline{m'}\,\overline{x'}-a_1\sin\left[\frac{2\pi}{\lambda}\left(\overline{x'}-c\overline{t'}\right)+\phi\right]. \tag{1a}$$

$$\overline{h_2'}\left(\overline{x'},\overline{t'}\right)= d+\overline{m'}\,\overline{x'}+a_2\sin\left[\frac{2\pi}{\lambda}\left(\overline{x'}-c\overline{t'}\right)\right]. \tag{1b}$$

Where a_1 and a_2 are the amplitudes of the wave lower and upper walls respectively, λ is the wavelength, c is the phase speed of the wave, $\overline{m'}$ $\left(\overline{m'}<<1\right)$ is the non–uniform parameter, the phase difference ϕ varies in the range $0\le\phi\le\pi$, $\phi=0$ corresponds to a symmetric channel with waves out of the phase i.e. both walls move towards the outward or inward simultaneously and further a_1, a_2, d and ϕ satisfy the condition for the divergence channel at the inlet of flow, otherwise both the walls collide.

$$a_1^2+a_2^2+2a_1a_2\cos\phi\le(2d)^2. \tag{2}$$

A. Couple Stress Fluid Model

For a couple stress fluids, the constitutive equations are represented by

$$\mathrm{T}_{ji,j}+\rho_f\,f_i=\rho_f\frac{dv_i}{dt},$$

$$e_{ijk}T_{jk}^{A}+M_{ji,j}+\rho_f C_i=0,$$

$$\overline{s'}_{ij}=-\overline{p'}\delta_{ij}+2\mu d_{ij},$$

$$\mu_{ij}=4\eta\varpi_{j,i}+\eta'\varpi_{i,j},$$

In the above equations, v_i is the velocity vector, C_i is the body moment per unit mass, f_i is the body force vector per unit mass, T_{jk}^{A} and e_{ij} are the antisymmetric and symmetric parts of the stress tensor T_{jk}, respectively, M_{ij} is the couple-stress tensor, μ_{ij} is the deviatoric part of M_{ij}, ϖ_i is the vorticity vector, d_{ij} is the symmetric part of the velocity gradient, μ is the viscosity of the fluid, $\overline{p'}$ is the pressure, δ_{ij} is the Kronecker delta, ρ_f is the density and η,η' are constantly associated with the couple stress fluid.

B. Governing Equations

The equations of continuity and momentum are given as follows:

$$\frac{\partial\overline{u'}}{\partial\overline{x'}}+\frac{\partial\overline{v'}}{\partial\overline{y'}}=0, \tag{3}$$

$$\rho_f\left(\frac{\partial\overline{u'}}{\partial\overline{t'}}+\overline{u'}\frac{\partial\overline{u'}}{\partial\overline{x'}}+\overline{v'}\frac{\partial\overline{u'}}{\partial\overline{y'}}\right)=-\frac{\partial\overline{p'}}{\partial\overline{x'}}+\mu\nabla^2\overline{u'}-\eta\nabla^4\overline{u'}, \tag{4}$$

$$\rho_f\left(\frac{\partial\overline{v'}}{\partial\overline{t'}}+\overline{u'}\frac{\partial\overline{v'}}{\partial\overline{x'}}+\overline{v'}\frac{\partial\overline{v'}}{\partial\overline{y'}}\right)=-\frac{\partial\overline{p'}}{\partial\overline{y'}}+\mu\nabla^2\overline{v'}-\eta\nabla^4\overline{v'}, \tag{5}$$

Where

$$\nabla^2=\frac{\partial^2}{\partial\overline{x'^2}}+\frac{\partial^2}{\partial\overline{y'^2}},\quad \nabla^4=\nabla^2\nabla^2$$

The following non-dimensional parameters are introduced in Equations (3-5),

$$x=\frac{\overline{x'}}{\lambda},\ y=\frac{\overline{y'}}{d},\ t=\frac{c\overline{t'}}{\lambda},\ u=\frac{\overline{u'}}{c},\ v=\frac{\overline{v'}}{c\delta},\ \delta=\frac{d}{\lambda},\ h_1=\frac{\overline{h_1'}}{d},\ h_2=\frac{\overline{h_2'}}{d}, \tag{6}$$

$$\mathrm{Re}=\frac{cd\rho_f}{\mu},\ m=\frac{\overline{m'}\lambda}{d},a=\frac{a_1}{d},b=\frac{a_2}{d},\gamma_1^2=\frac{c\mu^2}{\eta},\ p=\frac{d^2\overline{p'}}{c\lambda\mu}.$$

In which δ and Re represent the wave number and Reynolds number, respectively, whereas *a* and *b* are non-dimensional amplitudes of the lower and upper walls, respectively, and *m* is the non-uniform parameter. We finally get,

$$\mathrm{Re}\,\delta\left(\frac{\partial u}{\partial t}+u\frac{\partial u}{\partial x}+v\frac{\partial u}{\partial y}\right)=-\frac{\partial p}{\partial x}+\left(\delta^2\frac{\partial^2 u}{\partial x^2}+\frac{\partial^2 u}{\partial y^2}\right)-\frac{1}{\gamma_1^2}\left(\delta^2\frac{\partial^2}{\partial x^2}+\frac{\partial^2}{\partial y^2}\right)\left(\delta^2\frac{\partial^2 u}{\partial x^2}+\frac{\partial^2 u}{\partial y^2}\right), \tag{7}$$

$$\mathrm{Re}\,\delta^3\left(\frac{\partial u}{\partial t}+u\frac{\partial v}{\partial x}+v\frac{\partial v}{\partial y}\right)=-\frac{\partial p}{\partial y}+\delta^2\left(\delta^2\frac{\partial^2 v}{\partial x^2}+\frac{\partial^2 v}{\partial y^2}\right)-\frac{\delta^2}{\gamma_1^2}\left(\delta^2\frac{\partial^2}{\partial x^2}+\frac{\partial^2}{\partial y^2}\right)\left(\delta^2\frac{\partial^2 v}{\partial x^2}+\frac{\partial^2 v}{\partial y^2}\right), \tag{8}$$

In which the equation of continuity will be identically satisfied.

Under the hypothesis of long wavelength *(δ<<1)* and low Reynolds number assumptions, ignoring the terms δ and their higher orders in Equations (7-8), one can obtain,

$$\frac{\partial p}{\partial x}=\frac{\partial^2 u}{\partial y^2}-\frac{1}{\gamma_1^2}\frac{\partial^4 u}{\partial y^4}, \tag{9}$$

$$\frac{\partial p}{\partial y}=0, \tag{10}$$

$$u=0,\ \frac{\partial^2 u}{\partial y^2}=0 \text{ at } y=h_1=-1-mx-a\sin(2\pi(x-t)+\phi) \tag{11a}$$

$$u=0,\ \frac{\partial^2 u}{\partial y^2}=0 \text{ at } y=h_2=1+mx+b\sin(2\pi(x-t)) \tag{11b}$$

C. Rate of Volume Flow

Introduce the wave frame with the x and y coordinates to move in the x direction with wave velocity (c), and then the unsteady flow in the laboratory frame can be considered steady. The velocities and coordinates in the two frames are associated with

$$x=\overline{x'}-c\overline{t'},\ y=\overline{y'},\ u=\overline{u'}-c,\ v=\overline{v'} \tag{12}$$

Where u, v are the velocity components in the wave frame (x, y). The instantaneous flow volume rate $\overline{Q}\left(\overline{x'},\overline{t'}\right)$ in the frame stationary is given by

$$\overline{Q}\left(\overline{x'},\overline{t'}\right)=\int_{\overline{h_1'}(\overline{x'},\overline{t'})}^{\overline{h_2'}(\overline{x'},\overline{t'})}\overline{u'}\left(\overline{x'},\overline{y'},\overline{t'}\right)d\overline{y'} \tag{13}$$

in which $\overline{h_1'}$ and $\overline{h_2'}$ are the function of $\overline{x'}$ and $\overline{t'}$.

Substituting Equation (12) into Equation (13), we obtain,

$$\overline{Q}\left(\overline{x'},\overline{t'}\right)=\overline{q}+c\overline{h_2'}-c\overline{h_1'}$$

$$\text{where } \overline{q}=\int_{\overline{h_1'}}^{\overline{h_2'}}u(x,y)dy \tag{14}$$

is the rate of volume flow in the moving frame.

The time-averaged flow over a period $\left(T=\lambda/c\right)$ at a fixed position X is defined as

$$\overline{Q}=\frac{1}{T}\int_0^T Qd\bar{t}\ . \tag{15}$$

If we substitute Equation (14) into Equation (15) and integrate, we get

$$\overline{Q} = \overline{q} + a_1 c \sin\frac{2\pi}{\lambda}\left(\overline{x'} - c\overline{t'}\right) + a_2 c \sin\left[\frac{2\pi}{\lambda}\left(\overline{x'} - c\overline{t'}\right) + \phi\right]. \tag{16}$$

If we find the dimensionless mean flows (F), in the laboratory frame, wave frame and Θ according to

$$F = \frac{\overline{Q}}{cd}, \quad \Theta = \frac{\overline{q}}{cd}, \tag{17}$$

One finds that Equation (16) from, after applying Equations (6) and (17) we get [18, 19, 25]

$$F(x,t) = \Theta + a\sin 2\pi(x-t) + b\sin[2\pi(x-t) + \phi] \tag{18}$$

in which

$$F = \int_{h_1}^{h_2} u\,dy. \tag{19}$$

III. EXACT SOLUTION

The extract solution of the problem of Equations (9)-(11) is

$$u = \frac{1}{(\partial p/\partial x)}\left[A_4 + A_3 y + A_2\cosh(\gamma_1 y) + A_1\sinh(\gamma_1 y) + \frac{y^2}{2}\right],$$

The corresponding stream function is

$$\psi = \frac{\partial p}{\partial x}\left(A_4 y + \frac{A_3 y^2}{2} + \frac{A_2\sinh(\gamma_1 y)}{\gamma_1} + A_1\left(\frac{\cosh(\gamma_1 y) - 1}{\gamma_1}\right) + \frac{y^3}{6}\right),$$

Where the constant of integration is taken to be zero. Through Equation (19) we can find that

$$\frac{\partial p}{\partial x} = \frac{6\gamma_1 F}{\left(6\gamma_1 A_4(h_2 - h_1) + 3\gamma_1 A_3(h_2^2 - h_1^2) + 6A_2(\sinh(\gamma_1 h_2) - \sinh(\gamma_1 h_1)) + 6A_1(\cosh(\gamma_1 h_2) - \cosh(\gamma_1 h_1)) + \gamma_1(h_2^3 - h_1^3)\right)},$$

Where

$$A_1 = \frac{(\cosh(\gamma_1 h_2) - \cosh(\gamma_1 h_1))}{\gamma_1^2\sinh(\gamma_1(h_2 - h_1))},$$

$$A_2 = -\frac{(\gamma_1 A_1\sinh(\gamma_1 h_2) + 1)}{\gamma_1\cosh(\gamma_1 h_2)},$$

$$A_3 = \frac{2A_2(\cosh(\gamma_1 h_2) - \cosh(\gamma_1 h_1)) + 2A_1(\sinh(\gamma_1 h_2) - \sinh(\gamma_1 h_1)) + (h_2^2 - h_1^2)}{2(h_2 - h_1)},$$

$$A_4 = -\left(A_3 h_2 + A_2\cosh(\gamma_1 h_2) + A_1\sinh(\gamma_1 h_2) + (h_2^2/2)\right),$$

The non-dimensional expression for the pressure rise Δp is given as follows:

$$\Delta p = \int_0^1 \frac{\partial p}{\partial x}dx,$$

IV. RESULTS AND DISCUSSION

This category exposes the effects of different values of the geometrical parameters like amplitudes of lower and upper walls $(a \text{ and } b)$, couple stress fluid parameter (γ_1), phase difference (ϕ), non-uniform parameter (m) and the average-time mean-flow rate $(\overline{Q})$ on the velocity, the average rise in pressure per wavelength and trapping.

We have sketched Figures (2-5) to investigate the significance of the velocity distribution. Figure 2 clarifies the change of the velocity distribution of the fluid versus the width of the tapered asymmetric channel of various values of the couple stress fluid parameter (γ_1). One can observe from the figure that the velocity reduces as the couple-stress fluid parameter increases. Physiologically, it may be that the fluid flow of affected urine in the ureter due to suspended particles is blocked. In addition, in a wider part of the channel $y \in [-2.2, -1.2]$ and $y \in [0.6, 1.8]$, the variation in velocity is relatively small.

Figure 3 shows the consequence of the average time mean-flow rate $(\overline{Q})$. It shows the velocity of the fluid is parabolic in nature. In extension to that increase in the average mean flow rate $(\overline{Q})$ leads to reduce in the horizontal velocity (u). The excitement of the phase variation ϕ on the velocity is represented in Figure 4 with the fixed values of different parameters. It is evaluated that the velocity distribution of the fluid, in the essential part of the channel, decreases with increasing ϕ. The effects of the amplitude of the upper wall on the velocity are visible in Figure 5. This chart shows that expanding (a) results in an increase in the velocity of the fluid.

We have plotted Figures 6-9 to examine the significance of the amplitude distribution. An amplitude distribution is exposed to see the influence of different values of the amplitude of the upper wall (b), phase difference (ϕ), non-uniform parameter (m) and the couple stress parameter (γ_1) on the average rise in pressure (ΔP) versus the time average flow mean rate $(\overline{Q})$ with the exact values of other parameters involved in the expression of ΔP. The graph can be sectored four parts (i.e.) the right-hand upper quadrant (I) stand for the region of the peristaltic pumping wherein $\Delta P > 0$ and $\overline{Q} > 0$. Quadrant (II) represents increased flow when $\Delta p < 0$ and $\overline{Q} > 0$. Quadrant (IV) in which $\Delta P > 0$ and $\overline{Q} < 0$ is called backward or retrograde pumping. It obviously indicates that the relationship between ΔP and $\overline{Q}$ is a linear and that both of them have an inverse reciprocal relation. It is noticed from Figure 6 with a development in amplitude of upper wall *b*, the average rise in pressure decreases in peristaltic pumping. Moreover, free pumping $(\Delta P = 0)$ has become wider. Figure 7 reveals the relation between $\overline{Q}$ and Δp for various values of non-uniform parameter (m). One can discover that for the given ΔP, flux $\overline{Q}$ depend on *m* and it reduces to the extent of non-uniform parameter (m). We notice from Figure 8 that the pumping rate in peristaltic as well as in retrograde decreases when the phase difference (ϕ) is increased. Figure 9 gives the influence of couple-stress parameter γ_1 on ΔP. It is examined that an extended γ_1 result reduces the free pumping, peristaltic pumping and conflicting pressure gradient.

Trapping is one of the interesting phenomena in peristaltic flow. The formation of an internally circulating bolus in the region of closed streamlines is called trapping, and this trapped circulating bolus moves forward along the peristaltic wave frame. The trapping of non-uniform parameter (m), mean flux $(\overline{Q})$, and couple-stress fluid parameter (γ_1) are illustrated in Figure 10. The remarkable notice on the trapping aspect is that the appearance of a circulating bolus is present when fluid movement is the expansion/contraction of the asymmetric channel. In addition, it finds out that the volume of the trapped circulating bolus progresses with the progress of all the flow parameters m, $\overline{Q}$ γ_1.

V. CONCLUSIONS

The present investigation has discussed the peristaltic transport of a couple-stress fluid in the horizontal tapered asymmetric channel. The governing equations have been modeled and evaluated using long wavelength, and low Reynolds number approximations have been adopted. The correct expressions for horizontal pressure gradient, horizontal velocity and stream function are analytically determined. The main decisions of the present study are as follows:

1) The large values of Couple stress fluid parameter γ_1 correspond to that of a Newtonian fluid.
2) The magnitude of the velocity of a Newtonian fluid is higher than a couple-stress fluid.
3) The rate of peristaltic pumping decreases with increasing non-uniform parameter and couple stress fluid parameter.
4) The capacity of the circulating bolus rises with a raises of a non-uniform parameter.
5) In figure 11, we conclude that our results are in accordance with [19] when the amplitudes of both walls are equal and in the absence of the phase difference.

REFERENCES

[1] T.W. Latham, Fluid motion in a peristaltic pump, Cambridge: MS Thesis, MIT, 1966.
[2] Y.C. Fung, C.S. Yih, Peristaltic transport, J. App. Mech. 35 (1968) 669 - 675.
[3] A.H. Shapiro, M.Y. Jaffrin, S.L. Weinberg, Peristaltic pumping with long wavelengths at low Reynolds number, J. Fluid Mech. 37 (1969) 799 - 825.
[4] M.Y. Jaffrin, A.H. Shapiro, Peristaltic pumping, Annual Review of Fluid Mechanic, 3 (1971) 13 - 37.
[5] O. Eytan, D. Elad, Analysis of intra-uterine motion induced by uterine contractions, Bull. Math. Biol. 61 (1999) 221-238.
[6] M. Mishra, A. Ramachandra Rao, Peristaltic transport of a Newtonian fluid in an asymmetric channel, Z. Angew. Math. Phys. 54 (2003) 532-550.

[7] M. Kothandapani, S. Srinivas, Non-linear peristaltic transport of a Newtonian fluid in an asymmetric channel through a porous medium, Phys. Lett. A, 372 (2008) 1265-1276.
[8] D. Tripathi, A mathematical model for the peristaltic flow of chyme movement in small intestine, Math. Biosci. 233 (2) (2011) 90-97.
[9] C. Dhanapal, J. Kamalakkannan, J. Prakash, J. Kothandapani, Analysis of peristaltic motion of a nanofluid with wall shear stress, microrotation and thermal radiation effects, Appl. Bionics Biomech. 412374 (2016) 412374.
[10] J. Prakash, E.P. Siva, D. Tripathi, M. Kothandapani, Nanofluids flow driven by peristaltic pumping in occurrence of magnetohydrodynamics and thermal radiation, Mater. Sci. Semicond. Process. 100 (2019) 290-300.
[11] R. Vijayaragavan, P. Tamizharasi, A. Magesh, Brownian motion and thermoporesis effects of nanofluid flow through the peristaltic mechanism in a vertical channel, J. Porous Media, 25(6) (2022) 65-81.
[12] K.K. Raju, R. Devanathan, Peristaltic motion of a non-Newtonian fluid, Rheol. Acta. 11 (1972) 170-178.
[13] G. Radhakrishnamacharay, Long wave length approximation to peristaltic motion of a power law fluid, Rheol. Acta 21 (1982) 30-35.
[14] L.M. Srivastava, V.P. Srivastava, Peristaltic transport of blood: Casson model-II, J.Biomech. 17 (1984) 821-829.
[15] M. Kothandapani, J. Prakash, Effects of thermal radiation parameter and magnetic field on the peristaltic motion of Williamson nanofluids in a tapered asymmetric channel, Int. J. Heat Mass Transf. 81 (2015) 234-245.
[16] A. Magesh, M. Kothandapani, Heat and mass transfer analysis on non-Newtonian fluid motion driven by peristaltic pumping in an asymmetric curved channel, Eur. Phys. J. Spec. Top. 230 (2021) 1447-1464.
[17] A. Magesh, M. Kothandapani, V. Pushparaj, Electro-osmatic flow of Jeffery fluid in an asymmetric micro-channel under the effect of magnetic field, J. Phys. Conf. Ser. 1850 (2021) 012102.
[18] L.M. Srivastava, V.P. Srivastava, S.N. Sinha, Peristaltic Transport of a Physiological Fluid: Part I. Flow in Non-Uniform Geometry, Biorheol. 20 (1983) 153-166.
[19] L.M. Srivastava, V.P. Srivastava, Peristaltic Transport of a Power-Law Fluid: Application to the Ductus Efferentes of the Reproductive Tract, Rheol. Acta, 27 (1988) 428-433.
[20] V. K. Stokes, Couple stresses in fluids, Phys. Fluids, 9 (1966) 1709-1715.
[21] Kh. S. Mekheimer, Peristaltic transport of a couple stress fluid in a uniform and non-uniform channels, Biorehology, 39 (2002) 755765.
[22] Kh. S. Mekheimer, Effect of the induced magnetic field on peristaltic flow of a couple stress fluid, Phys. Lett. A, 372 (2008) 4271-4278.
[23] S. K. Pandey, M. K. Chaube, Study of wall properties on peristaltic transport of a couple stress fluid, Meccanica, 46 (2011) 1319-1330.
[24] S. Nadeem, S. Akram, Peristaltic flow of a couple stress fluid under the effect of induced magnetic field in an asymmetric channel, Arch. Appl. Mech. 81 (2011) 97-109.
[25] J. Kamalakkannan, C. Dhanapal, M. Kothandapani, non–Linear peristaltic flow of power-law fluid in the tapered asymmetric channel, International Journal for Research in Applied Science and Engineering Technology, 11 (01) (2023) 1545-1554.

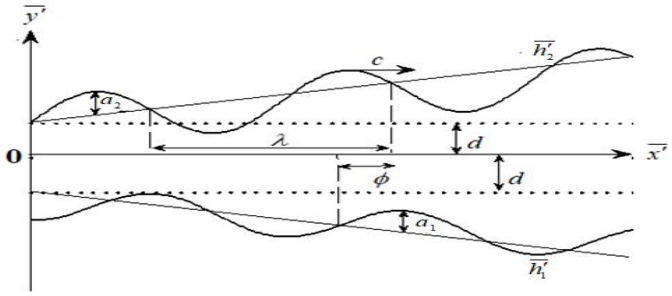

Figure 1 Schematic depiction of fluid flow induced by a horizondal tapered asymmetric channel

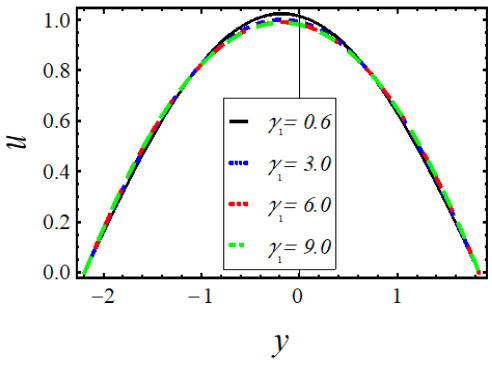

Figure 2 Velocity distribution of γ_1

$a = 0.3, b = 0.7, \gamma_1 = 1.5, x = 0.4, t = 0.2, \phi = \pi/4$

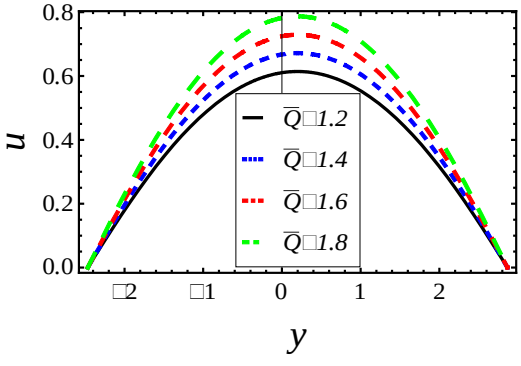

Figure 3 Velocity distribution of $\bar{Q}$

$a = 0.6, b = 0.5, \bar{Q} = 1.8, x = 0.2, t = 0.1, \phi = \pi/4$

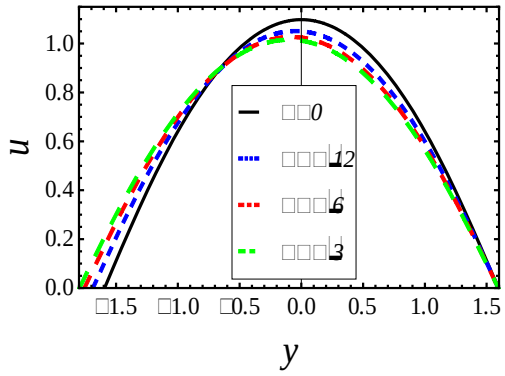

Figure 4 Velocity distribution of ϕ

$a=0.5, b=0.5, \overline{Q}=1.7,\ x=0.1,\ t=0,\ \gamma_1=1.5$

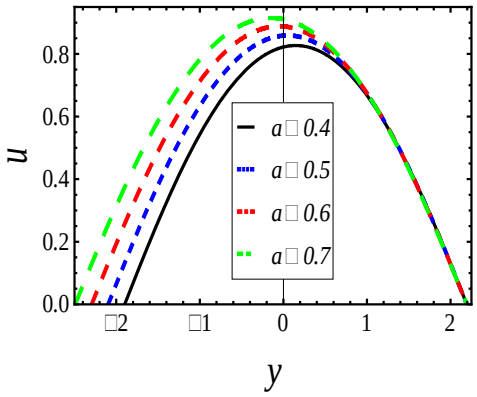

Figure 5 Velocity distribution of a

$b=0.7, \overline{Q}=1.9,\ x=0.3,\ t=0.2,\ \gamma_1=1.5, \phi=\pi/4$

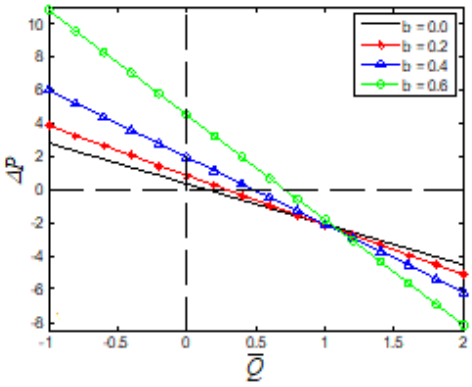

Figure 6 Pressure rise versus flow rate for b

$a=0.4,\ b=0.7,\ \gamma_1=5, \phi=\pi/4$

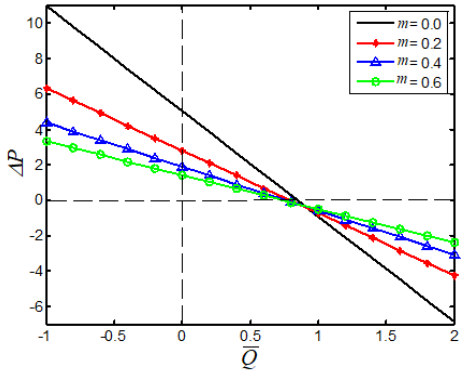

Figure 7 Pressure rise versus flow rate for m

$a=0.4, m=0.1,\ \gamma_1=1.5, \phi=\pi/6$

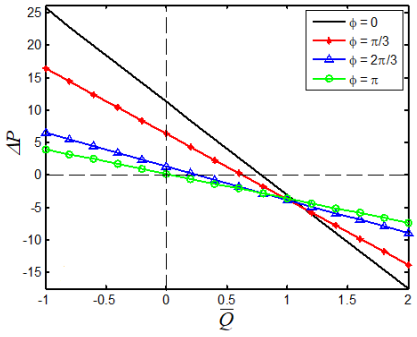

Figure 8 Pressure rise versus flow rate for ϕ

$a=0.4,\ b=0.5,\ m=0.1, \phi=\pi/4$

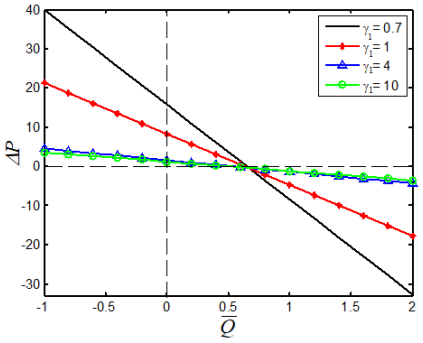

Figure 9 Pressure rise versus flow rate for γ_1

$a=0.6,\ b=0.4,\ \gamma_1=1, m=0.2$

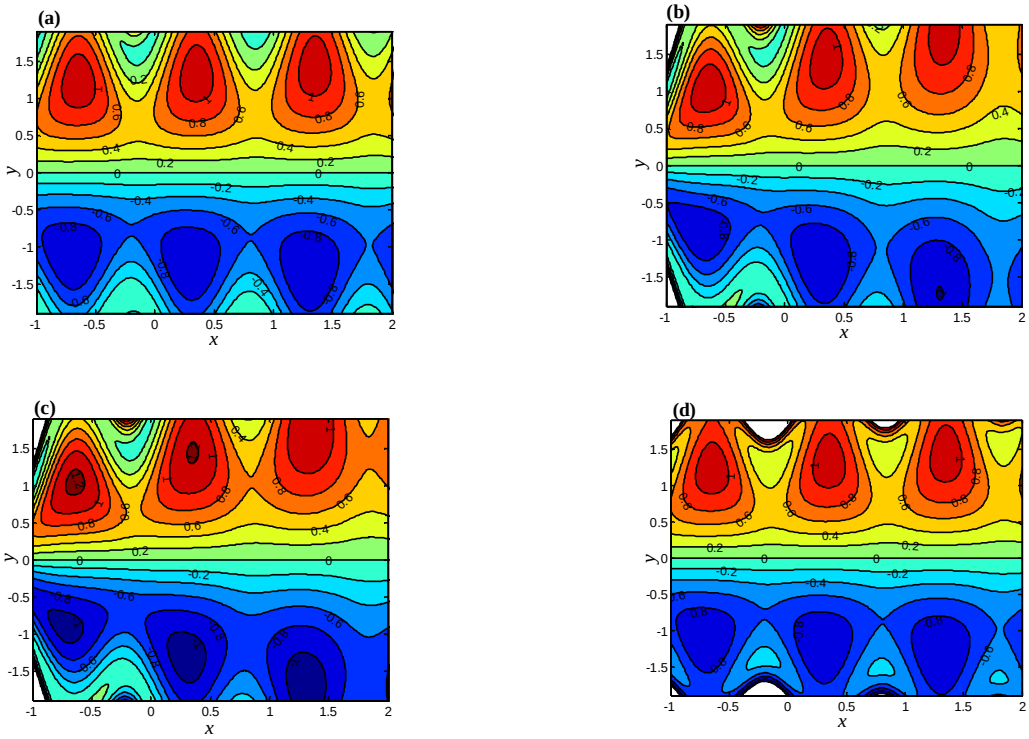

Figure 10 Streamlines for $\overline{Q}=1.6,\ m=0.1,\ \gamma_1=0.5$ (panel (a)), $\overline{Q}=1.6,\ m=0.4,\ \gamma_1=0.5$ (panel (b)), $\overline{Q}=1.8,\ m=0.4,\ \gamma_1=0.5$ (panel (c)), $\overline{Q}=1.6,\ m=0.1,\ \gamma_1=4$ (panel (d)). The other parameters chosen $a=0.2,\ b=0.3,\ t=0.1,\phi=\pi/12$

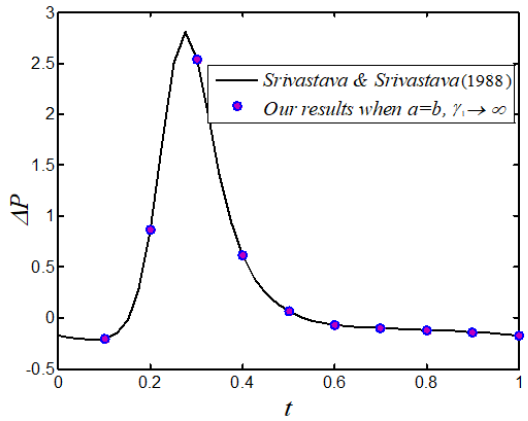

Figure 11 Validation of present study with Srivastava and Srivastava [19]

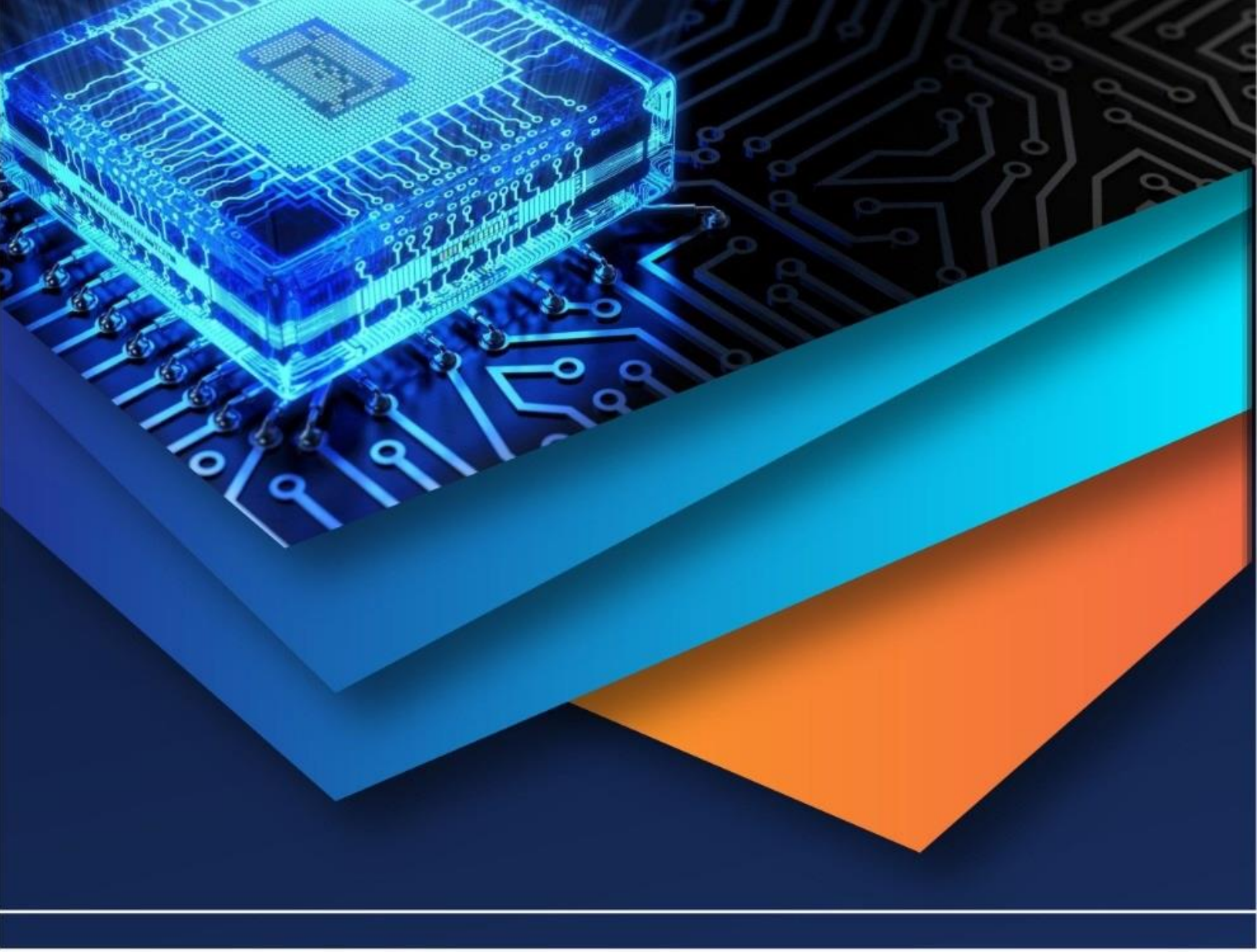

10.22214/IJRASET

45.98

IMPACT FACTOR: 7.129

IMPACT FACTOR: 7.429

INTERNATIONAL JOURNAL FOR RESEARCH

IN APPLIED SCIENCE & ENGINEERING TECHNOLOGY